Accurate Bolt Tightening Using Model-Free Fuzzy Control for Wind Turbine Hub Bearing Assembly

Christian Deters, Hak-Keung Lam, *Senior Member, IEEE*, Emanuele Lindo Secco, Helge A. Würdemann, Lakmal D. Seneviratne, *Member, IEEE*, and Kaspar Althoefer, *Member, IEEE*

***Abstract*— In the modern wind turbine industry, one of the core processes is the assembly of the bolt-nut connections of the hub, which requires tightening bolts and nuts to obtain well-distributed clamping force all over the hub. This force deals with nonlinear uncertainties due to the mechanical properties and it depends on the final torque and relative angular position of the bolt/nut connection. This paper handles the control problem of automated bolt tightening processes. To develop a controller, the process is divided into four stages, according to the mechanical characteristics of the bolt/nut connection: a fuzzy logic controller (FLC) with expert knowledge of tightening process and error detection capability is proposed. For each one of the four stages, an individual FLC is designed to address the highly nonlinearity of the system and the error scenarios related to that stage, to promptly prevent and avoid mechanical damage. The FLC is implemented and real time executed on an industrial PC and finally validated. Experimental results show the performance of the controller to reach precise torque and angle levels as well as desired clamping force. The capability of error detection is also validated.**

***Index Terms*— Bolt tightening, fuzzy logic control, industrial fuzzy logic control, sensor-based tightening.**

I. Introduction

WIND turbine industry is one of the most promising technologies within renewable energies field, compared with other ones like solar energy. Power generation through wind has reached a mature technology level, good infrastructure, and convinces with regards to cost competitiveness [1]; wind energy is likely to play an essential role in the future for replacing a number of currently used energy sources [2]. Predictions outline that wind energy may supply 12% of the overall world's demand in the near future, meaning that turbines will be more powerful and wind parks are likely to see turbines with increased rotor diameters [3], [4].

Research into wind turbine manufacturing is an important topic with a number of challenges and potentially far-reaching ramifications in a fast-developing market. One critical process of wind turbine manufacturing is the hub assembly process [5]. Essential to hub assembly is successfully creating accurate bolt-nut connections between the blades bearings and the main hub component (Fig. 1); hub assembly is currently performed manually by workers employing torque wrenches, hydraulic tensioning tools and gauges [6]. The assembly process requires to be completed with high precision, according to strict specifications—bolts improperly tightened to a faulty level or those suffering from mechanical damage are to be avoided and such failure scenarios are to be detected early on in the assembly process.

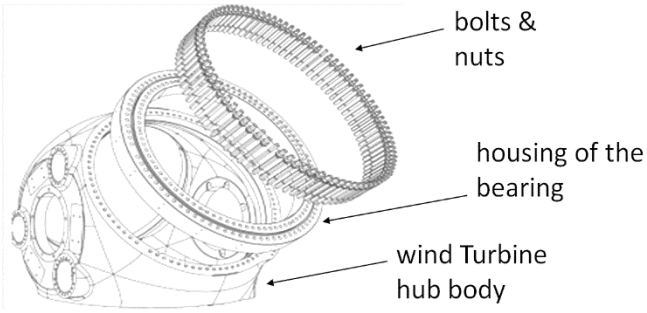

Fig. 1. Overall assembly process (picture provided by Gamesa Corp.).

Although hub assembly is usually conducted by human workers, some research on automating the bolt-tightening process has been conducted. Current control strategies on bolt tightening are based on the concept of proportional-integral-derivative (PID) control, and, in some cases, combined with torque/angle tightening technique [7]. In general, PID controllers are well accepted within industrial applications and exhibit high performance on linear systems. However, the tightening process exhibits nonlinearities and uncertainties due to mechanical friction between the bolt and nut threads, variations of environmental temperature, presence of physical damages on threads [8]–[13]. Therefore, a simple PID controller with fixed values of proportional, integral, and derivative gains may not provide sufficient level of tightening performance [14].

This motivates the use of alternative techniques like model-free fuzzy logic controllers (FLCs), which demonstrate a better capability to deal with uncertainties and nonlinearities [15]–[24]. Model-free FLCs allow employing expert knowledge on tightening and even detection of failure scenarios such as cross treading, screw jamming, slippage, and misalignments during the tightening process [7], [18], [25]–[30]. It is noted that in a model-based approach, problems like variation of friction, material properties variation, bolt size, and installation alterations would require different models for each case, which

Manuscript received January 13, 2014; accepted February 13, 2014. Manuscript received in final form March 3, 2014. This work was supported by the European Community, Seventh Framework Programme under Grant FP7-NMP-2009-SMALL-3 and Grant NMP-2009-3.2-2 through the EU Project COSMOS under Grant 246371-2. Recommended by Associate Editor H. Gao.

The authors are with the Department of Informatics, King's College London, London WC2R 2LS, U.K. (e-mail: c.deters@outlook.de; hak-keung.lam@kcl.ac.uk; emanuele.secco@kcl.ac.uk; helge.wurdemann@kcl.ac.uk; lakmal.seneviratne@kcl.ac.uk; k.althoefer@kcl.ac.uk).

Digital Object Identifier 10.1109/TCST.2014.2309854

cannot be easily and precisely included within a numerical model.

A theoretical FLC concept addressing all nonlinear components of screw fastening has been presented in [19]. However, this latter paper is not using the introduced four-stage tightening strategy—as indeed has been proposed in [31]—to address the specific nonlinear components of the bolt system. On the contrary, these ones can be controlled by the introduced model-free approach; in addition, an approach like the one reported in [19], does not provide error recognition and targets industrial integration. Moreover, the tightening tool runs on different rotational speeds to avoid damages in critical phases of the process. It is noted that the approach proposed here includes error detection—an idea that was also explored by others with regards to a range of dynamically operated systems, including motor control, wind energy conversion, winch drive, and screw fastening [16], [25], [30], [32], [33], allowing early detection of common error scenarios based on torque/angle tightening information [7], [34].

This paper investigates bolt-tightening based on a practical manufacturing situation. In view of the complexity of the system and control process, a model-free Mamdani-type FLC [26]–[28], [35], [36], which allows the integration of expert knowledge with the control methodology, is employed to serve as a controller for the control of: 1) the output torque and 2) the angle of the bolt-tightening tool. To facilitate the design of the FLC, the process is divided into four stages according to mechanical properties, such as thread size and type, bolt material, and washer size [37]. Knowledge on each stage is employed to establish a rule base and membership functions for the FLC. As an individual fuzzy controller is designed for each stage, nonlinearity can be clearly addressed and utilized for control design to improve the performance of the overall system [29], [35], [38]–[40]. To realize the fuzzy error detector for each stage, knowledge on potential error scenarios such as misalignment of the nut on the bolt, mechanical damages of the bolt or the nut, incorrect thread types and sizes are defined in linguistic rules based on Mamdani FLC. Since different wind turbine hubs define different tightening specifications, the parameters within the FLC can be changed according to the assembly specifications to achieve the specified torque/angle. The proposed FLC, error detector, and status determiner are implemented on a real-time industrial control system. Experiments are conducted to show the merits of the proposed control scheme.

This paper is organized as follows. Section II shows the nut assembly process, which are divided into four stages supporting the design of the FLC and error detector. Section III introduces the tightening stages and the FLC. Section IV presents the experimental results. The conclusion is drawn in Section V.

II. Materials and Methods

A. Wind Turbine Assembly and Bolt Tightening

The wind turbine hub is made of three main parts, which are the hub, the bearing, and the pitch system. The bearings are assembled using up to 128 bolts (depending on the wind turbine hub) to connect them to the hub (Fig. 1).

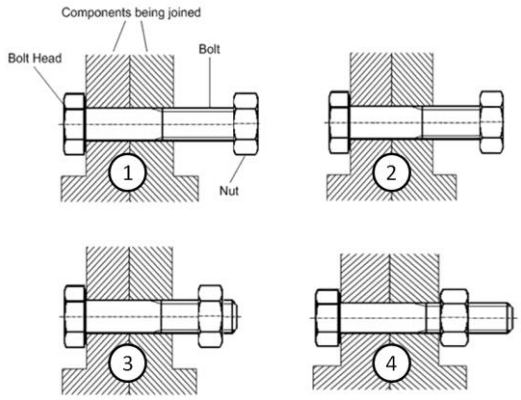

Fig. 2. Four stages of the bolt tightening process [17], [18].

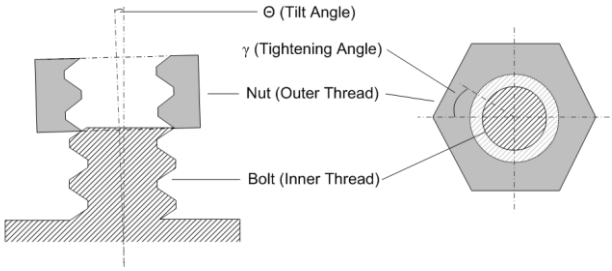

Fig. 3. Alignment problems.

B. Sequence of Bolt Tightening

The sequence for bolt tightening is essential for accurate tightening as well as for assembly error detection. The process has been analyzed and it can be subdivided into four different stages. Stage 1 regards the initial bolt/nut alignment. This will subsequently lead to partial and full engagement (Stages 2 and 3, respectively) of the bolt and the nut; finally, as soon as the nut will touch the flange, the system starts Stage 4, which is the final part of the tightening process.

1) Stage 1—Bolt/Nut Alignment: At the beginning of the tightening process, the female and male threads of the bolt and the nut meet at their starting point (Fig. 2, top left panel). In this stage, the requirement for the controller is to provide a slow start to avoid possible damages to the threads of the bolt and nut in case a jamming situation arises and to apply the required torque levels within a specific low range of their relative angular position. Since the bolt has a round shape, misalignment situations may arise and cause damage (Fig. 3), therefore, in such a situation, the assembly should be promptly stopped and the bolt replaced. This also may happen in another error scenarios such as if a wrong bolt is used, e.g., with a thread type different from that of the nut. Therefore, the aim of this stage is to move the nut into a specified angle and to assure a proper alignment between the nut and bolt avoiding all of the aforementioned errors.

2) Stage 2—Partial Engagement: The nut is tightened for a few degrees ensuring that both bolt and nut threads are touching each other (Fig. 2, top right panel). This match requires a small value of applied torque to overcome the friction caused by the two threads being in contact. Possible error scenarios of this stage include three types of cross

threads: 1) in the nut; 2) in the top region of the bolt; and 3) due to different thread types. In this case, continuing the tightening may lead to a jamming situation, and, in turn, may cause to an unexpected and unwanted higher torque level.

Another possible error is due to bolt/nut misalignment: in Fig. 3, the tilt angle Θ refers to misplacement originating, for example, from a wrong automatic pick and place process. Angle Θ should be zero, otherwise the nut may get jammed. It is noted that tightening angle γ describes the tightening angle range and depends on the assembly specification.

3) Stage 3—Full Engagement: At this stage, the nut is running down until reaching the flange and a maximum and steady friction level occurs (Fig. 2, bottom left panel). Possible errors include cross threads on the bolts shaft and dirt between the threads, which can be detected by unexpectedly high torque (HT). Monitoring the angular displacement of the nut is very important in this phase, since it contains feedback about how far the nut has been traveled along the bolt shaft. Moreover, this information aids the estimation of the effective bolt length (as detailed in the assembly specifications) and—based on the travelled distance of the nut—the detection of wrong or missing washers.

4) Stage 4—Final Bolt Tightening: The final part of the tightening process starts as soon as the nut has reached the flange. Turning the nut during this part of the tightening process generates the desired clamping force between the flange and the nut (Fig. 2, bottom right panel). The torque level as well as the final angular position of the nut are provided within the assembly specifications. Accordingly, the requirement of this stage is to apply appropriate values of torque within well-defined angular displacements and without exceeding the bolt tension limit (TL), since otherwise errors would occur.

C. Control Architecture

A Mamdani FLC was setup, incorporating expert knowledge resulting in a set of rules, the four-stage bolt-nut tightening process was created. According to [35], the overall controller structure is

$$\mathrm{MAMD}(x, y) = \bigvee_{i=1}^{n} (A_i(x) \text{ and } B_i(y)) \tag{1}$$

where A_i and B_i are the fuzzy numbers [e.g., low angle (AL) and desired angles] as a listening of n-possibilities. In (1), the fuzzy numbers can be seen as x is A_1 and y is B_1 or x is A_2 and y is B_2, and so on. Fuzzy rules can be integrated as conjunction of implications

$$\mathrm{RULES}(x, y) = \bigwedge_{i=1}^{n} (A_i(x) \rightarrow B_i(y)). \tag{2}$$

In (2), the rules have been set as a listening of n possibilities: if x is A_1 then y is B_1 and x is A_2 then y is B_2.

The FLC inputs and outputs are tightening tool angular position (measured by means of an integrated encoder) and torque (measured using integrated strain gauge sensor), respectively (Fig. 4). A further input, error signal is used for TL detection, which monitors the velocity of the torque (if it becomes constant the plastic region is reached). The output is a voltage signal in the ± 10 V range, which sets the tool spinning speed; an additional tension limit input is introduced, which is linked to the torque velocity (if the velocity is constant and the angle increases, the plastic region of the bolt has been reached). The control error, namely the difference between the real torque/angle and their desired values, is minimized using the membership functions—which define the targeted control values and error values, and the linguistic rules—within the FLC block. Therefore, no additional error feedback is shown within the controller scheme (Fig. 4) and the torque/angle values are directly fed into the controller.

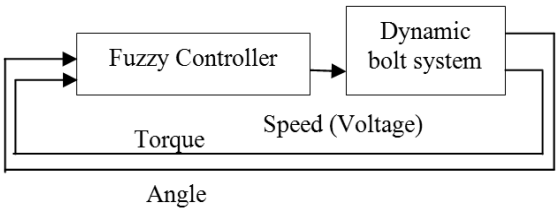

Fig. 4. Generic control diagram used for all Stages 1–4.

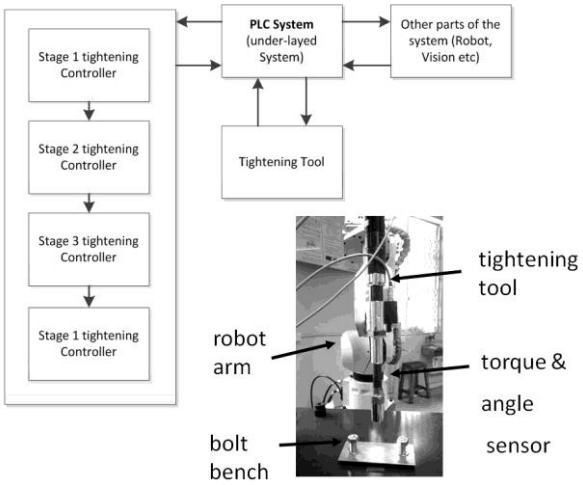

Fig. 5. Overall controller architecture.

Since this application is to be used within an industrial environment, the architecture use a programmable logic controller (PLC) system [41], which integrates MATLAB/Simulink programming language (Mathworks Inc.) within a real-time Beckhoff TwinCAT 3 software automation system [42]. In our setup, the PLC is connected to an Industrial Fanuc M6iB Robot arm, which is equipped with a DSM BL 57/140 MDW tightening tool attached to the end-effector flange (Fig. 5). A bolt bench with three bolts is used to simulate the bolt tightening process (Fig. 5).

The FLC is cyclically executed to exchange data with the PLC, which is connected with the tool. Control signals are sent back to the PLC in real-time; we note two important advantages:

1) different FLCs can be selected by the same PLC, according to different bolt types;
2) multiple tools can be integrated by calling the FLC several times.

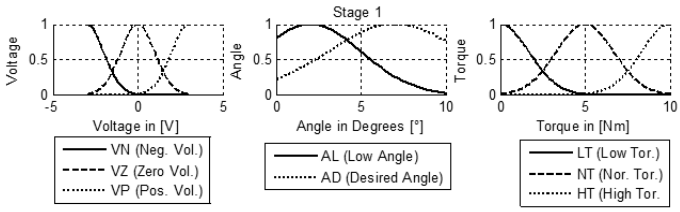

Fig. 6. Membership functions of Stage 1.

TABLE I
LINGUISTIC RULES FOR STAGE 1

INPUTS		OUTPUTS	
Angle	Torque	Voltage	Error
AL	LT	PV	F
AL	NT	PV	F
AL	HT	ZV	T
AD	LT	ZV	F
AD	NT	ZV	F
AD	HT	ZV	T

1) Stage 1 Control Strategy (Bolt/Nut Alignment): An multiple-input, multiple-output FLC with two inputs, torque and angle as sensing inputs, and two outputs, voltage for setting the tool's speed and an signal for reporting an error scenario, has been designed. To define the angle and torque levels, an experiment has been carried out to estimate the values for a normal completion of Stage 1. It turned out that the nut is aligned after c. 7° at a torque level of c. 5 Nm. If a misalignment occurs, the angle level cannot be reached by applying the normal torque (NT), as the nut is jammed. Based on these experimental verified levels, the membership functions defined in Stage 1 defined.

In Stage 1, the input torque of the FLC contains three Gaussian membership functions named *"low torque (LT)", "normal torque (NT)"* and *"high torque (HT)"*; the input angle contains two membership functions, which are called *"low angle (AL)"* and *"desired angle (AD)"*; the output voltage contains three membership functions, namely *"negative voltage (VN)", "zero voltage (VZ)"* and *"positive voltage (VP)"*. All membership functions are in the Gaussian shape, as shown in Fig. 6.

The fuzzy rule set is reported in Table I, where the fourth column refers to the output of the fuzzy error detector, which generates either a true (T) status, indicating an erroneous condition, or a false (F) status, indicating proper operation. In the first case, the FLC switches off the output voltage and reports an error output by sending a supervisory signal to the PLC. During operation, the tightening tool rotates until it reaches the starting position (where the bolt and the nut thread meet); then the torque slightly increases and the control target of Stage 1 is satisfied.

2) Stage 2 Control Strategy (Partial Engagement): Stage 2 FLC has a structure similar to the previous one, with the membership functions of the angle adapted to the desired angular range (Fig. 7), such that if a high torque scenario

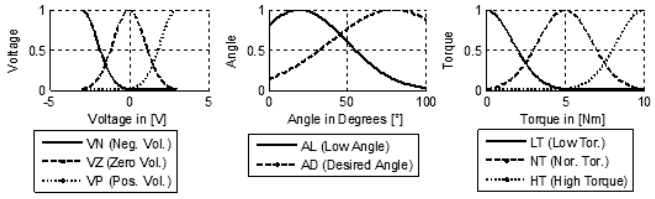

Fig. 7. Membership functions of Stage 2.

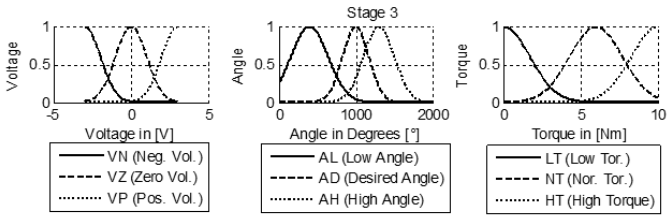

Fig. 8. Membership functions of Stage 3.

arises, the voltage output is set to zero and an error output is returned. The membership functions are linked using the same linguistic rules as reported in Table I and the section describing Stage 1. Stage 2 is entirely angle-based, since only three to five entire turns of the nut are required for this stage to complete.

It is noted that the angle levels of the membership functions for Stage 2 are 10 times higher. This level has also been estimated experimentally to ensure the nut is in the desired position to continue to Stage 3. The torque level stays the same, as only in an error scenario the torque will go up—it is only monitored to detect error scenarios.

3) Stage 3 *Control Strategy (Full Engagement):* In Stage 3, the FLC contains also two inputs (torque and angle for sensing) as well as two outputs (the voltage and error signal for actuation), as in the previous stages. Compared with Stage 1, the angle range has to be redefined to cover the expected run down angle range of the bolt's shaft down to the washer/flange; moreover the error detector has to identify any possible high torque scenarios, which may be caused by cross threads on the shaft (caused by a low angle and a high torque scenario). Accordingly, the membership functions have been specified, as shown in Fig. 8.

Due to the presence of friction between the bolt and the nut, the baseline of the torque value within the fuzzy rules have to be increased (as the nut's thread is now fully set on the bolt's thread) and furthermore the angle region has to be redefined to estimate whether a correct washer has been installed (a missing or false washer would cause a high angle scenario) and to include the target angle. A high torque scenario within the low angle region would be indicative of a problem (as the situation of a cross thread on the bolt or too short a bolt being installed) and must stop the tightening action. According to all these concerns, more membership functions and linguistic rules have to be defined within this stage, as shown in Table II.

Stage 3 is also entirely angle based, as the control target is to run the nut down to the washer/flange. The angle has been estimated based on experimental results and may be modified for different bolt sizes. The torque level is increased as the nut is now completely on the bolts thread, which increases

TABLE II
LINGUISTIC RULES FOR STAGES 2 AND 3

INPUTS		OUTPUTS	
Angle	Torque	Voltage	Error
AL	LT	PV	F
AL	NT	PV	F
AL	HT	ZV	T
AD	LT	ZV	F
AD	NT	ZV	F
AD	HT	ZV	T
AH	LT	ZV	T
AH	NT	ZV	T
AH	HT	ZV	T

the friction. Experiments showed that the applied torque is around 7-Nm maximum.

4) Stage 4 Control Strategy (Tightening Process): The FLC in Stage 4 tightens the nut to the final desired torque and within a specified and desired angular range. Here, the TL has to be preserved (meaning that the bolt cannot be over tightened, possibly due to a wrong bolt installation). Therefore, the controller is setup using three sensing inputs (torque, tension-limit, and angle) and two outputs (voltage to set the tool speed and one supervisory signal for the error and tension-limit detection). Two comparators have been implemented with experimentally estimated thresholds, which are linked to the tightening and tensioning limit output respectively, this setup enables the error and TL detection.

Three membership functions are assigned to each of the inputs. The error recognition should detect if the bolt reaches its TL due to a deviation of the torque from the allowed range of torque levels; as soon as the torque velocity remains constant and the angle is still increasing, the plastic region of the bolt has been reached and the tightening process must stop, either with an error (if the torque has not been reached) or with no error (if the torque has been reached and the angular position is within the desired range).

Furthermore, in this stage, the FLC returns to the PLC system whether the process has been successfully completed or not. According to these observations, the membership functions for the tension limit are implemented in addition to the membership functions introduced in Fig. 9: *reached tension limit (RT)*, *"close tension limit (CL)",* and functions are also introduced.

The outputs of the tightening (TIGH) and of the tension limit (TL) are supervisory signals set by the FLC then a set of 27 linguistic rules has been set up to cover the required actions (Table III) based on all possible input scenarios and outputs. The overarching system (factory control system) receives an error signal, which is either true in an error scenario or false if the process has been completed without errors, the current stage is transferred as well.

Combining all membership functions and linguistic rules, the overall FLC shape is obtained, as shown in Fig. 10.

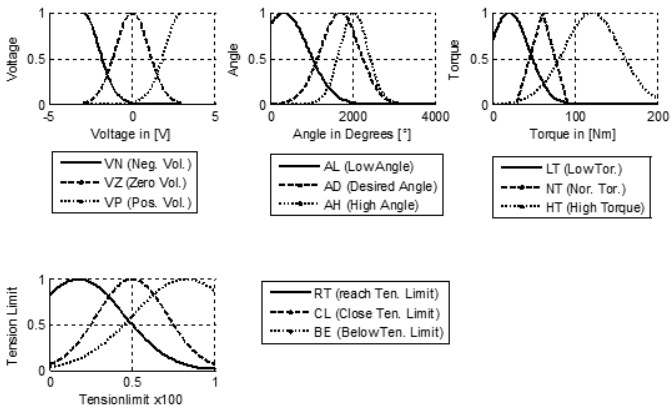

Fig. 9. Membership functions of Stage 4.

TABLE III
STAGE 4 LINGUISTIC RULES

INPUTS			OUTPUTS		
Torque	Angle	Tension Limit	Voltage	TIGH	TL
LT	AL	BE	VP	T	BE
LT	AD	BE	VP	T	BE
LT	AH	BE	VP	T	BE
DT	AL	BE	VP	T	BE
DT	AD	BE	VZ	F	BE
DT	AH	BE	VZ	F	BE
HT	AL	BE	VP	T	BE
HT	AD	BE	VN	T	BE
HT	AH	BE	VN	T	BE
LT	AL	CL	VP	T	CL
LT	AD	CL	VP	T	CL
LT	AH	CL	VZ	F	CL
NT	AL	CL	VP	T	CL
NT	AD	CL	VZ	F	CL
NT	AH	CL	VZ	F	CL
HT	AL	CL	VP	T	CL
HT	AD	CL	VZ	F	CL
HT	AH	CL	VZ	T	CL
LT	AL	RT	VZ	F	RT
LT	AD	RT	VZ	F	RT
LT	AH	RT	VZ	F	RT
NT	AL	RT	VZ	F	RT
NT	AD	RT	VZ	F	RT
NT	AH	RT	VZ	F	RT
HT	AL	RT	VZ	F	RT
HT	AD	RT	VZ	F	RT
HT	AH	RT	VZ	F	RT

III. VALIDATION

A. Experiment Setup

The previous section introduced a four-stage FLC performing bolt tightening with error detection. To validate the system in an industrial software and hardware environment, the controller was initially implemented using the MATLAB/SIMULINK Programming Language and then imported into the Beckhoff TwinCAT 3 system using MATLAB coder. The controller is then executed at a cycle frequency of 2 kHz (i.e., with a cycle time of 500 μs). This cycle time was selected due to the speed requirement of the tightening process.

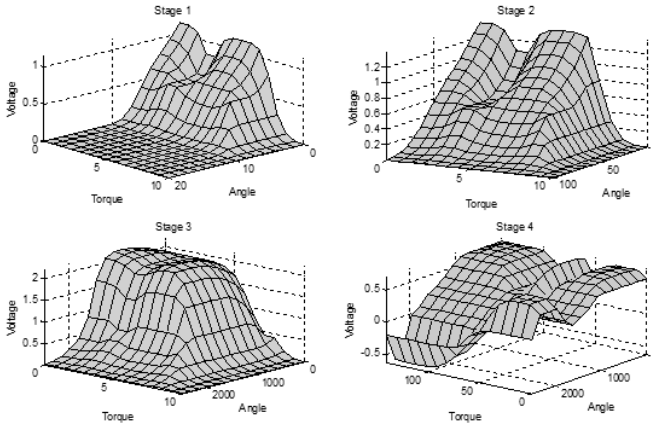

Fig. 10. From the top left to the bottom right panel, the s Stages 1–4 membership functions with their linguistic rules, respectively.

The tightening tool (model DSM BL 57—maximum torque performance of 140 Nm) was mounted on the end-effector of a Fanuc M6i-B robot arm; during a regular tightening procedure, the robot picks an M24 nut and places it on the top of M24 bolt; the rotational tightening speed was controlled by a voltage command, whereas an optical encoder and torque sensor—both integrated within the tool-measured angle and torque levels, respectively. The inputs to the FLC were the acquired angle and torque values, while the FLC outputs were the voltage control signals driving the tool motor and an error signal, reporting on the type of experienced error scenario.

A washer sensor (MecSense KMR 50 KN), for measuring the clamping force, was inserted between the nut and the flange to measure the effective performance of the tightening process. Generally, the clamping force depends on multiple factors like the applied torque, the relative angular positions between the bolt and nut threads, the geometric and mechanical characteristics of their contact surfaces to name a few [18]. Usually, this washer sensor is not installed in the physical assembly line and is only used here for verification of our approach.

B. Validation Scenarios

Several tightening processes were performed, as well as sessions for testing the error detection capabilities of our algorithm. In particular, to test the error detection capabilities, diverse error scenarios were set up during the tightening processes. The error feedback is setup using a Boolean flag within the PLC, which returns the actual torque, angle and stage values as soon as an error is detected.

The performance of the FLC was also compared with the performance of a classical industrial PID controller often employed for bolt tightening.

C. Error Recognition Performance

To validate the controller and its capability to detect the errors, six experimental sessions were performed involving different error scenarios (S). For regular tightening (S1), 30 trials have been conducted to show the accuracy of the FLC

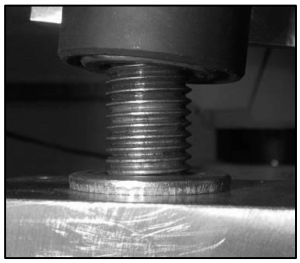

Fig. 11. Misalignment error. The robot places the nut on a faulty angle, which causes the nut to be stuck on the bolt as soon as tightening process is started.

and compare it with a PID controller. For the error detection (S2–S6), eight trials have been conducted on each scenario to demonstrate the error detection capabilities. At the beginning of each trial, the tightening tool loaded the nut and was positioned in front of the bolt; then, the controller was started and executed until completing the tightening process or any error detection occurred.

The desired torque level is depending on the application's specification. In wind turbine manufacturing, HT values are usually required during hub. Based on the specifications, the PLC sets the membership function parameters for the desired torque and angle and starts the controller.

Six scenarios (S1–6) (listed below) replicating typical errors occurring while an operator performs bolt tightening during wind turbine assembly are investigated. Furthermore, these scenarios were conceived and designedto possibly cover diverse corresponding error detections within the four stages of the tightening process. These are the six scenarios that were experimentally validated.

1) Regular Tightening (S1): No error detection was expected within this scenario, since a correct M24 nut was positioned on the tightening tool and in front of an M24 bolt.

2) Misalignment Error (S2): The tool and the nut were erroneously positioned with respect to the bolt, to replicate the misalignment error (Fig. 11); the error detection was expected to occur at Stage 1.

3) Jamming Error (S3): A nonmetric nut was tightened on an M24 bolt; the error was expected to be detected at Stage 2, since the torque level would rise up to an undesirable level at this stage. The threads of the nut and the bolt were also expected not to grab one into the other, due to their different geometric shapes.

4) Insertion of Two Washers (S4): In this scenario, one additional washer was added on top of the original washer used (Fig. 12) and the system was expected to recognize its presence during the Stage 3 or early Stage 4 because the torque level would rise to too high a value within Stage 3 and would stay at that overly high level at a low angle in Stage 4.

Fig. 12 shows a two washers' scenario. In this condition, the tightening angle cannot be reached according to the assembly specifications; therefore, the torque level increases before a specified angle is reached and an error is detected.

5) Missing Nut (S5): To simulate a mistake of the operator, the nut was removed from the tightening tool (Fig. 13). In this situation, the controller error detection was foreseen to occur

Fig. 12. Two washers error scenario. The second washer will cause an error detection within Stage 3 or 4, since the desired angular position of the nut will not be reached.

Fig. 13. Missing nut scenario: the tool is touching the washer as soon as it is placed on the nut, because of the missing nut.

at Stage 3, because no increase in the torque was expected and the angle is expected to increase in value without bounds, in Stage 3. As shown in the last figure, the tightening tool spins on the bolt as there is no nut, which causes an increase of the torque value. This should cause an error since the controller is expecting a rise in the torque within the Stage 3, at comparatively low angular values. Finally, the nut runner is touching and spinning on the washer since there is no nut in this particular setup.

6) Wrong Bolt Versus Nut (S6): The proper M24 nut was replaced with an inappropriate M14 nut too small. In this condition, the controller runs into Stage 3, as the torque level remains on a low level and the wrong bolt error should finally occur at Stage 3. This type of error can also imply that too small a nut-runner was installed. In this scenario, the nut will not be picked and placed as the tool cannot pick it.

During all the experimental tests, the following two parameters were used to measure the system performance:

1) percentage of successful detection within all the trials of the session, namely the number of trials (out of all trials) in which at least one error message was detected;
2) percentage of successful detection within all the trials of the session and within the expected stage of the tightening process, namely the number of trials (out of all trials) in which the error message occurred within the proper and expected Stage.

IV. Result

A. Scenario 1—Regular Tightening

In this experiment, the control target is to reach a final torque value of 60 Nm as well as a tightening angle of approximately 2000°. The angle value may change according to the installation of the bolt, which could lead to different

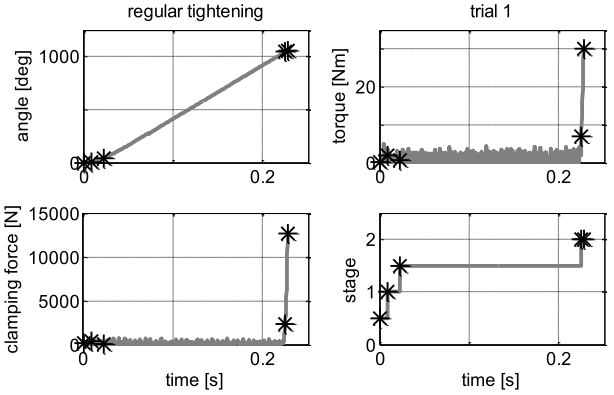

Fig. 14. One trial (out of 30) of regular tightening (S1): from top left to bottom right panel, the angle, torque, clamping force, and stage time patterns, respectively. Black stars report the stage transitions.

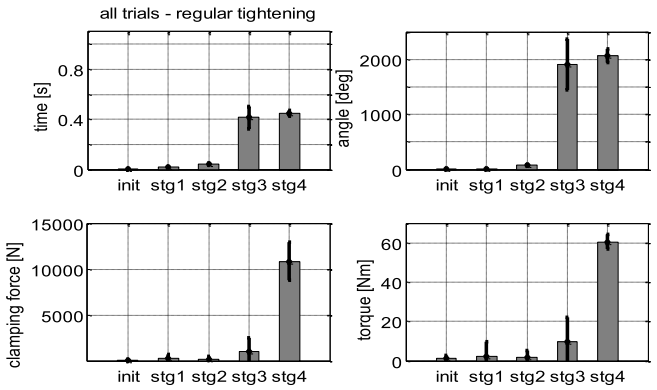

Fig. 15. Average distribution (in gray colored bars) and two times standard deviations (black lines) of regular tightening (Scenario 1): from top left to bottom right panel, the time, angle, clamping force, and torque respectively.

starting angles of the bolt thread, depending on how the operator positions the bolt in the hole.

It needs to be considered that only this scenario has been compared with the PID controller as only this scenario targets the complete Tightening process with no errors. The sessions concerned with error detection scenarios are not included in the PID tests.

Fig. 14 summarizes the typical time history of the angle, torque, clamping force, stage, and error signal during the trials within the error-free tightening scenario (S1): the five black stars report the stage transitions, namely the beginning of the trial, the end of first, second, third, and fourth stages and the trial end (first, second to fifth, and last markers, respectively); in the bottom right panel of the figure, the relevant stage and the transition process is shown.

As reported within Fig. 15, from the results of the experimental data of S1, it can be summarized that:

1) the complete regular (error-free) tightening process took less than 0.5 s to be completed within the four stages;
2) the process is always completed with no error detection;
3) at the end of Stage 4, the average value of the tightening torque is always very close to the target value of 60 Nm (bottom right panel, Fig. 15), whereas the angular position is largely distributed around 2000° (top right panel, Fig. 15)—the latter is mainly due to the variations in the initial installation of the bolt;

TABLE IV
REGULAR TIGHTENING FLC: MEAN AND TWO TIMES STANDARD DEVIATION OF TIME, ANGLE, CLAMPING FORCE, AND TORQUE AT EACH STAGE TRANSITION

	INIT	END OF STAGE 1	END OF STAGE 2	END OF STAGE 3	END OF STAGE 4
time [s]	0.001 ± 0.000	0.018 ± 0.002	0.046 ± 0.002	0.414 ± 0.089	0.446 ± 0.024
angle [°]	0.111 ±0.667	8.000 ± 0.000	82.444 ± 1.764	1908.000 ± 455.500	2066.000 ± 115.37
clamping force [N]	69.338 ± 76.360	245.335 ± 450.532	178.753 ± 335.286	994.063 ± 1543.632	10853.478 ± 2120.509
Torque [Nm]	1.238 ± 1.419	2.094 ± 7.670	1.973 ± 3.454	9.765 ± 12.159	60.253 ± 1.05

4) the magnitude of the clamping force is 13.5 KN on average (bottom left panel of Fig. 15). This is the average targeted clamping force employing our torque/angle tightening algorithm;
5) the stage-by-stage time transition distribution is quite regularly distributed on Stages 1 and 2, whereas it is more extended on Stages 2 and 3 (top left panel, Fig. 15). This is due to the run-down phase of the nut when it is driven down to the flange due to uncertainties in the angle and thread (the starting point varies).

To quantify these observations, the mean and two times standard deviations values of time, angle, torque, and clamping force were calculated at each stage transition and are shown in Fig. 14 and Table IV.

These results reflect and match the effective targets of the membership functions of the FLC, and in particular as follows.

1) The averaged time at which each stage transition occur is equal to 0.018, 0.046, 0.414, and 0.446 s at the end of Stages 1–4, respectively (Table IV); the two times standard deviation is always less than 5.4% of the average, except from the beginning of Stages 2 and 4 (11.2% and 21.5%, respectively).
2) At the end of the Stage 1, the distribution of the angular position is quite large, because of the trial by trial differences of the initial mechanical alignment between the tightening tool and the nut with respect to the bolt; remarkably, no variability of the angle is found at beginning of Stage 2 ($8 \pm 0°$) and during the other transitions the percentage of variation reduces less than 6%, except from the beginning of Stage 4 (23.9%).
3) The clamping force is the results of the combinations of multiple nonlinear factors and therefore it is quite hard to be predicted. Nevertheless, a significantly low distribution of the clamping force is registered at the end of the tightening (19.5%), meaning that—because of the FLC—the process is highly repeatable (i.e., the controller succeeds in dealing with uncertainties). This latter result is a clear sign of the system's capability to achieve the desired tightening force at the appropriate angular position of the nut with respect to the bolt and flange, with an error distribution between 6% and 5.8%, respectively.

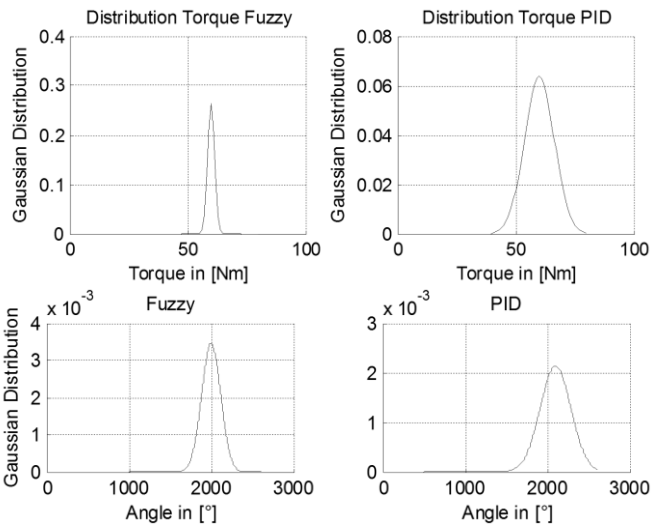

Fig. 16. Comparison of the FLC versus the PID controller in terms of final torque of regular tightening during 30 trials (left and right panels, respectively).

These fuzzy controller results were compared with the results of a PID controller, where the proportional, derivative and integral gains were obtained by trial and error. The PID controller was employed for all four stages during 30 trials of regular (error-free) tightening. The average results of both the fuzzy and PID controllers are modeled by a Gaussian distribution of the final torque and angle, Fig. 16. It is noted that the PID controller results depend on how the gains are setup and may need to be reset, if the bolt system changes.

As it can be observed from the computed Gaussian distributions, the accuracy of the FLC on the desired torque level is higher than the one of the PID controller. In fact, the mean $\pm$ standard deviation of the FLC torque and angle are equal to 60.253 ± 1.5 Nm and $2066° \pm 115.37°$, respectively, whereas the same parameters of the PID controller are equal to 61.10 ± 6.5 Nm and $2100° \pm 184°$, respectively. As mentioned before, this is due to the uncertainty of the start angle of the bolt thread, which varies depending on how it is installed. The FLC can address this issue using expert knowledge incorporated in its rule base and membership functions. The final value is within a tolerance band and may be further improved upon by introducing additional rules and membership functions; nevertheless, this approach may make the design of the FLC more complex and therefore increasing its computational cost.

Fig. 16 shows that the confidence level for the FLC is higher and, hence, the FLC is more reliable.

Furthermore, five more experiments have been conducted using 70 Nm and 2100° as target values. Indirectly, the control target is the clamping force, which normally cannot be measured in real time during the tightening process in a real industrial setting, hence, in the assembly line, there will be no sensor washer to measure the clamping force.

Fig. 17 shows the resulting clamping force after completion of the tightening process. The time delay is caused as the nut runs down from Stages 1–4. The times may differ from the

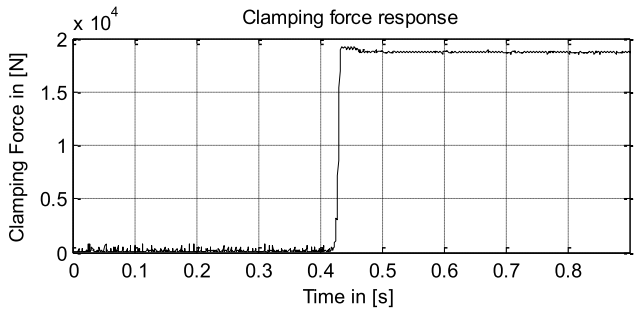

Fig. 17. Final result for the clamping force.

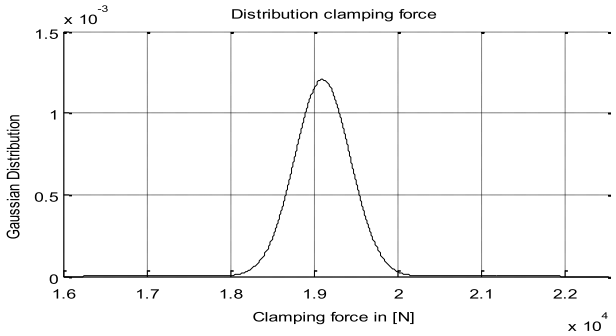

Fig. 18. Gaussian distribution of five experiments for 70 Nm, 2100°.

previous experiments, since two new target values have been selected for torque and angle values.

During the tightening process, the bolt gets twisted; the more torque is Applied, the further the bolt is twisted [19]. As soon as the tightening process is completed, the material relaxes, which means that the nut moves slightly back from its position (until it gets stopped by the friction between the flange, washer, and the nut). This is also effecting the clamping force (Fig. 17).

Fig. 18 shows the Gaussian distribution for five experiments at the end of the settling effect. It can be seen that the clamping force can be reached without too much deviation, even though it cannot be controlled directly in real time using the torque/angle tightening technique [16]. It is a result of the final torque and the angle values.

B. Scenario 2—Misalignment Error

During all the trials of S2, the controller properly detected all the misalignments scenarios (100% of performance) and all these errors were detected within the proper stage, namely Stage 1 (Table VI). At the error event, the average and two times standard deviations of the angle, and torque were registered, while no clamping force was detected because of the expected and early stop of the tool at Stage 1. All detections were discovered within the first 0.01 s (namely, 0.005 ± 0.007 s) of the tightening process, with the tool having rotated less than 1° and a torque of only 12.1 ± 4.8 Nm being applied.

Table VI describes the error detection distribution in [%] over each stage. It can be seen that the error has been detected

TABLE V
AVERAGE AND TWO TIMES STANDARD DEVIATIONS OF THE TIME, ANGLE, CLAMPING FORCE (WHERE AVAILABLE), AND TORQUE AT ERROR DETECTION VALUES ARE MEAN ± TWO TIMES STANDARD DEVIATION

ERROR SCENARIOS	TIME [S]	ANGLE [°]	CLAMPING FORCE [N]	TORQUE [Nm]
S2: misalignment	0.005 ± 0.007	0.700 ± 0.966	-	12.143 ± 4.842
S3: jamming	0.016 ± 0.016	7.200 ± 5.147	-	2.032 ± 5.098
S4: 2 washers	0.331 ± 0.010	1481.000 ± 41.070	1618.320 ± 2243.610	12.880 ± 16.060
S5: missing M24 nut	0.484 ± 0.055	2101.300 ± 2.119	156.107 ± 484.998	0.043 ± 3.385
S6: big nut	0.481 ± 0.071	2081.60 ± 129.042	92.748 ± 349.256	0.952 ± 4.255

for each scenario. The PID Controller has not been tested on this scenario, as it does not include error detection capabilities.

C. Scenario 3—Jamming Error

All the jamming events were discovered within eight trials (100% of performance) while the detections occurred within the expected stage (i.e., Stage 2) in seven out of eight cases (90% of performance—see Table VI): in fact, during one of the trials, the error was found before entering in the expected stage, possibly due to the jamming occurring at the moment that the nut was placed on the bolt top (i.e., when the bolt's and nut's threads started to interact with each other) or a nut blockage as soon as the bolt's and nut's threads meet. As shown in Table V, all the error events were detected within the first 0.03 s from the beginning of the process, with the tool having rotated less than 15° and a torque load lower than 10 Nm (i.e., 17% of the maximum applied torque). Again, the PID Controller has not been tested in this scenario, as it does not include error detection capabilities.

D. Scenario 4—Insertion of Two Washers

In this scenario, two washers were placed, as shown in Fig. 12 and the tightening process was started. The controller exhibited a 100% performance over all the nine trials. This error was detected within the expected stage (i.e., Stage 3), in three out of nine trials (33% of performance); in all the other six trials, it was detected at the beginning of the Stage 4; because during seven trials, the nut and washers touched the flange, the variability of the clamping force was spread out more than in other scenarios (139%), whereas transition time and angle were well centered around their averaged values (3%) and the deviation of the torque settled at a value of 125%. Similar to Fig. 15, a representative figure of the time history of all the parameters during the insertion two washers' scenario is shown in Fig. 19.

As for all the other scenarios, the PID controller has not been tested in this scenario as it does not include error detection capabilities.

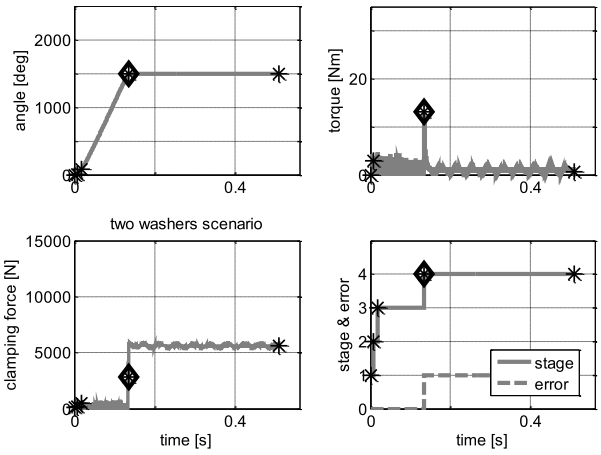

Fig. 19. Two washers' error detection occurring at Stage 4 during one trial (out of nine).

TABLE VI
PERCENTAGE OF SUCCESSFUL DETECTION OVERALL THE TRIALS AND WITHIN EACH STAGE WHERE THE ERROR WAS EXPECTED FOR EACH SCENARIO

ERROR SCENARIOS	DETECTION [%]	DETECTION STAGE [%]			
		Stage 1	Stage 2	Stage 3	Stage 4
S2:misalignment	100	100	-	-	-
S3: jamming	100	10	90	-	-
S4: 2 washers	100	-	-	33	67
S5: missing M24 nut	100	-	-	100	-
S6: small bolt, big nut	100	-	-	100	-

E. Scenario 5—Missing Nut

The missing nut was found in all the trials (100% of performance) and within the expected stage, namely the third one (100% of performance—Table VI). Table V reports the time history of the average values of the angle, clamping force, torque, and error during one representative trial. Consistent with the membership functions of the FLC, a very low variability of the angle was found (0.1%), whereas the distribution of the torque and, as a consequence, of the clamping force, was rather high. However, since the desired torque and angle values will never be reached—because of the missing nut—the large distributions can be ignored. Again, the PID controller has not been tested in this scenario, as it does not include error detection capabilities.

F. Scenario 6—Wrong Bolt Versus Nut

Within this scenario, a 100% of performance was registered both in terms of the detection of the error within all trials and within the expected stage (Stage 3). Table V reports the average values and their double standard deviation at the time of the detection. Similarly to the S5 results, a small variability of the angle was found (6.2%), whereas the distribution of the torque and of clamping force were large (377% and 447%, respectively).

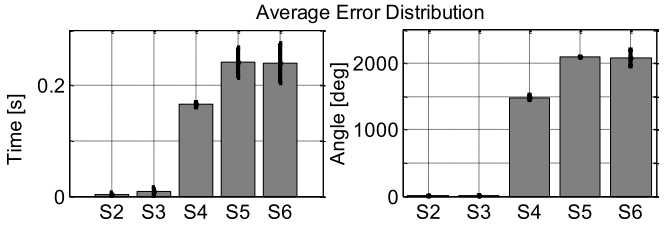

Fig. 20. Average distribution (in gray colored bars) and two times standard deviations (black lines) of the time and angle over all the different error scenarios S2÷6 (left and right panels, respectively) based on Table V.

In summary, Fig. 20 shows the average times and angles for all error Scenarios, which have been reported in this paper. The figure shows when and where the errors were detected in terms of time and angular position, respectively. The scenario tests have only been applied to the FLC-based approach and not on the PID controller.

V. CONCLUSION

This paper investigates bolt tightening in the framework of wind turbine hub assembly. The wind turbine hub contains of up to 128 bolts, which are used to mount the bearing onto the hub. The assembly process requires to be completed with a high level of accuracy concerning the final clamping force.

The process under investigation is a highly nonlinear one with uncertainties (such as variations in friction, angle, environment, and bolt/nut material). Errors need to be detected at an early stage to avoid any damage and to ensure that the assembly is completed according to the requirements and specifications.

To address this issue, a model-free FLC has been designed and implemented, based on a physical system analysis. According to the analyzed uncertainties, such as the variations of frictions and angles, the tightening process has been subdivided into four stages to include specific knowledge about the tightening operation for each of the stage and also to integrate error recognition so that the FLC can return an error feedback signal at the stage the error, such as misalignment occurs.

Results have been compared with a standard industry PID controller. It has been shown experimentally that the new four-stage FLC performs better overall in terms of final accuracy, and, in contrast to standard PID controllers, provides error detection capabilities, allowing an emergency stop to be initiated, when an error occurs. In particular, the FLC is implemented on a real-time industrial control system and showed the following performance:

1) the whole tightening process is completed in less than 0.5 s for regular tightening;
2) the accuracy of the FLC on the desired torque levels is more accurate than the one of the PID controller (60.253 ± 1.5 Nm versus 61.10 ± 6.5 Nm, respectively);
3) the accuracy of the FLC on the desired angular values is higher than the one of the PID controller ($2066° \pm 115.37°$ versus $2100° \pm 184°$, respectively).

Finally, in terms of error detection, the experimental results show that the FLC is capable to detect all the error scenarios within less than 0.5 s, avoiding any physical damage.

REFERENCES

[1] G. M. Joselin Herbert, "A review of wind energy technologies," *Renew. Substainable Energy Rev.*, vol. 11, no. 6, pp. 1117–1145, 2007.

[2] C. S. Ezio, "Exploitation of wind as an energy source to meet the world's electricity demand," *J. Wind Eng. Ind. Aerodyn.*, vols. 74–76, pp. 375–387, Apr. 1998.

[3] F. Yao, "Theory, desin and applications," in *Handbook of Renewable Energy Technology*. Singapore: World Scientific, 2011, pp. 3–20.

[4] R. Saidur, "A review on global wind energy policy," *Renew. Substainable Energy Rev.*, vol. 14, no. 7, pp. 1744–1762, 2010.

[5] C. Deters, H. A. Würdemann, J. S. Dai, L. D. Seneviratne, and K. Althoefer, "Reconfigurable assembly approach for wind turbines using multiple intelligent agents," in *Proc. Adv. Reconfigurable Mech. Robots I*, 2012, pp. 95–103.

[6] M. Sharpe, *Robotic Fabrication of Wind Turbine Power Generators*. YMN, Japan: FANUC Robot., 2009.

[7] (2013, Feb. 3). *Bolt Tightening Handbook*. SKF Eng., Shanghai, China [Online]. Available: http://www.skf.com/files/880426.pdf

[8] Y. Maeda and M. Iwasaki, "Initial friction compensation using rheology-based rolling friction model in fast and precise positioning," *IEEE Trans. Ind. Electron.*, vol. 60, no. 9, pp. 3865–3876, Sep. 2013.

[9] J. H. J. Potgieter and M. J. Kamper, "Torque and voltage quality in design optimization of low-cost non-overlap single layer winding permanent magnet wind generator," *IEEE Trans. Ind. Electron.*, vol. 59, no. 5, pp. 2147–2156, May 2012.

[10] H. Chaoui and P. Sicard, "Adaptive fuzzy logic control of permanent magnet synchronous machines with nonlinear friction," *IEEE Trans. Ind. Electron.*, vol. 59, no. 2, pp. 1123–1133, Feb. 2012.

[11] T. Yokoyama, M. Olsson, S. Izumi, and S. Sakai, "Investigation into the self-loosening behavior of bolted joint subjected to rotational loading," *Eng. Failure Anal.*, vol. 23, pp. 35–43, Jul. 2012.

[12] H. A. Talebi and K. Khorasani, "A neural network-based multiplicative actuator fault detection and isolation of nonlinear systems," *IEEE Trans. Control Syst. Technol.*, vol. 21, no. 3, pp. 842–851, May 2013.

[13] D. A. Dirksz and J. M. A. Scherpen, "Power-based set point control: Experimental results on a planar manipulator," *IEEE Trans. Control Syst. Technol.*, vol. 20, no. 5, pp. 1384–1391, Sep. 2012.

[14] K. H. Ang, G. Chong, and Y. Li, "PID control system analysis, design and technology," *IEEE Trans. Control Syst. Technol.*, vol. 13, no. 4, pp. 559–576, Jun. 2005.

[15] J. Villagra, V. Milanes, J. Perez, and C. Gonazalez, "Model free control techniques for Stop & Go systems," in *Proc. 13th IEEE Annu. Conf. Intell. Transp. Syst.*, Sep. 2010, pp. 1899–1904.

[16] H. Hanao, S. M. J. R. Fatemi, G. A. Capolino, and S. Sieg-Zieba, "Wire rope fault detection in a hoisting winch system by motor torque and current signature analysis," *IEEE Trans. Ind. Electron.*, vol. 58, no. 5, pp. 1727–1736, May 2011.

[17] E. L. Secco and G. Magenes, "A feedforward neural network controlling the movement of a 3-DOF finger," *IEEE Trans. Syst., Man Cybern., A, Syst. Humans*, vol. 32, no. 3, pp. 437–445, May 2002.

[18] N. Dhayagude, G. Zhiqiang, and F. Mrad, "Fuzzy logic control of automated screw fastening," *Robot. Comput.-Integr. Manuf.*, vol. 12, no. 3, pp. 235–242, 1996.

[19] S. Izumi, T. Yokoyama, A. Iwasaki, and S. Sakai, "Three-dimensional finite element analysis of tightening and loosing mechanism of threaded fastener," *Eng. Failure Anal.*, vol. 12, no. 4, pp. 604–615, 2005.

[20] T. Fujinaka, H. Nakano, and S. Omatu, "Bolt tightening control using neural networks," *IEEE Trans. Syst., Man, Cybern.*, vol. 3, no. 3, pp. 1390–1395, Oct. 2001.

[21] L. D. Seneviratne, F. A. Ngemoh, S. W. E. Earles, and K. A. Althoefer, "Theoretical modelling of the self-tapping screw fastening process," *Proc. Inst. Mech. Eng., C, J. Mech. Eng. Sci.*, vol. 215, no. 2, pp. 135–154, 2001.

[22] H. A. Mintsa, R. Venugopal, J.-P. Kenne, and C. Belleau, "Feedback linearization-based position control of an electrohydraulic servo system with supply pressure uncertainty," *IEEE Trans. Control Syst. Technol.*, vol. 20, no. 4, pp. 1092–1099, Jul. 2012.

[23] K. Althoefer, L. D. Seneviratne, P. Zavlangas, and B. Krekelberg, "Fuzzy navigation for robotic manipulators," *Int. J. Uncertainty, Fuzziness Knowl.-Based Syst.*, vol. 6, no. 2, pp. 179–188, 1998.

[24] H. K. Lam, H. Li, C. Deters, H. Würdemann, E. L. Secco, and K. Althoefer, "Control design for interval type-2 fuzzy systems under imperfect premise matching," *IEEE Trans. Ind. Electron.*, vol. 61, no. 2, pp. 956–968, Feb. 2014.

[25] B. Akin, C. Seungdeog, U. Orguner, and H. A. Toliyat, "A simple real-time fault signature monitoring tool for motor-drive-embedded fault diagnosis systems," *IEEE Trans. Ind. Electron.*, vol. 58, no. 5, pp. 1990–2001, May 2011.

[26] B. U. Xuhui, H. Zhongsheng, and J. Shangtai, "A statistical analysis of model free adaptive control with measurements disturbance," in *Proc. 29th Chin. Control Conf.*, Jul. 2010, pp. 2175–2181.

[27] H. A. Malki, L. Huaidong, and C. Guanrong, "New design and stability analysis of fuzzy proportional-derivative control system," *IEEE Trans. Fuzzy Syst.*, vol. 2, no. 4, pp. 245–254, Nov. 1994.

[28] M. Sugeno and K. Tanaka, "Successive identification of a fuzzy model and its application to prediction of a complex system," *Fuzzy Sets Syst.*, vol. 42, no. 3, pp. 315–334, 1991.

[29] H. K. Lam and M. Narimani, "Quadratic stability analysis of fuzzy model based control systems using staircase membership functions," *IEEE Trans. Fuzzy Syst.*, vol. 18, no. 1, pp. 125–137, Feb. 2010.

[30] K. Althoefer, B. Lara, Y. H. Zweiri, and L. D. Seneviratne, "Automated failure classification for assembly with self-tapping threaded fastening using artificial neural networks," *Proc. Inst. Mech. Eng., C, J. Mech. Eng. Sci.*, vol. 222, no. 6, pp. 1081–1095, 2008.

[31] F. Ngemoh, "Modeling the automated screw insertion process," Ph.D. dissertation, Dept. Eng., King's College, Univ. London, London, U.K., 1997.

[32] E. Kamal, A. Aitouche, R. Ghorbani, and M. Bayart, "Fuzzy scheduler fault-tolerant control for wind energy conversion systems," *IEEE Trans. Control Syst. Technol.*, vol. 22, no. 1, pp. 119–131, Jan. 2014.

[33] B. T. Thumati, G. R. Halligan, and S. Jagannathan, "A novel fault diagnostics and prediction scheme using a nonlinear observer with artificial immune system as online approximator," *IEEE Trans. Control Syst. Technol.*, vol. 21, no. 3, pp. 596–578, May 2013.

[34] C. Deters, E. L. Secco, H. A. Würdemann, H. K. Lam, L. D. Seneviratne, and K. Althoefer, "Model-free fuzzy tightening control for bolt/nut joint connections of wind turbine hubs," in *Proc. IEEE ICRA*, May 2013, pp. 270–276.

[35] P. Hajek. (2012 Jun. 13) *Fuzzy Logic* [Online]. Available: http://plato.stanford.edu/entries/logic-fuzzy/

[36] J. R. Marden, S. D. Ruben, and L. Y. Pao, "A model-free approach to wind farm control using game theoretic methods," *IEEE Trans. Control Syst. Technol.*, vol. 21, no. 4, pp. 1207–1214, Jul. 2013.

[37] M. Klingajay, L. D. Seneviratne, and K. Althoefer, "Identification of threaded fastening parameters using the Newton Raphson method," in *Proc. IEEE/RSJ Int. Conf. Intell. Robots Syst.*, Oct. 2003, pp. 2055–2060.

[38] A. Pisano, A. Davila, L. Fridman, and E. Usai, "Cascade control of PM DC drives via second-order sliding mode technique," *IEEE Trans. Ind. Electron.*, vol. 55, no. 11, pp. 3846–3854, Nov. 2008.

[39] F. H. F. Leung, H. K. Lam, S. H. Ling, and P. K. S. Tam, "Optimal and stable fuzzy controllers for nonlinear systems based on an improved genetic algorithm," *IEEE Trans. Ind. Electron.*, vol. 51, no. 1, pp. 172–182, Feb. 2004.

[40] C. Westermayer, R. Priesner, M. Kozek, and R. Bauer, "High dynamic torque control for industrial engine test beds," *IEEE Trans. Ind. Electron.*, vol. 60, no. 9, pp. 3877–3888, Sep. 2012.

[41] (2013, Jan. 2). *Phoenix Contact PC Works*. Phoenix Contact, Blomberg, Germany [Online]. Available: http:// www.phoenixcontact.com

[42] (2013, Jan. 2). *Beckhoff TwinCAT 3*. Beckhoff, Westphalia, Germany [Online]. Available: www.beckhoff.de

Christian Deters received the Dipl.Ing. degree in computer science from Hochschule Bremen, Bremen, Germany, and the M.Sc. degree from King's College London, London, U.K., in 2008 and 2009, respectively, where he is currently pursuing the Ph.D. degree.

His current research interests include control, automation, and manufacturing.

Hak-Keung Lam (M'98–SM'10) received the B.Eng. (Hons.) and Ph.D. degrees from the Department of Electronic and Information Engineering, Hong Kong Polytechnic University, Hong Kong, in 1995 and 2000, respectively.

He has been with King's College London, London, U.K., since 2005, where he was a Lecturer and is currently a Senior Lecturer. He is the co-editor for two edited volumes *Control of Chaotic Nonlinear Circuits* (World Scientific, 2009) and *Computational Intelligence and Its Applications* (World Scientific, 2012), and the co-author of the book *Stability Analysis of Fuzzy-Model-Based Control Systems* (Springer, 2011). His current research interests include intelligent control systems and computational intelligence.

Dr. Lam is an Associate Editor for the IEEE TRANSACTIONS ON FUZZY SYSTEMS and the *International Journal of Fuzzy Systems*, and serves on the editorial boards of several journals.

Emanuele Lindo Secco received the M.Sc. degree in mechanical engineering from the University of Padua, Padua, Italy, and the Ph.D. degree in bioengineering and medical computer science from the University of Pavia, Pavia, Italy, in 1998 and 2001, respectively.

He is currently a Research Associate with the Centre for Robotics Research, Department of Informatics, King's College London, London, U.K. His current research interests include robotics, biomimetic systems, sensor integration, and wearable sensors.

Helge A. Würdemann received the Dipl.Ing. degree in electrical engineering from the Leibniz University of Hanover, Hannover, Germany.

He was with the Auckland University of Technology, Auckland, New Zealand, in 2006, and with Loughborough University, Loughborough, U.K., in 2007, where he carried out a research project. He is currently a Research Associate with the Centre for Robotics Research, Department of Informatics, King's College London, London, U.K. His Ph.D. project, which he started in 2008, at King's College London was funded by the Engineering and Physical Sciences Research Council. In 2011, he was with the Research Team of Prof. K. Althoefer, involved in two European Union Seventh Framework Program projects. His current research interests include medical robotics for minimally invasive surgery and self-adaptive control architectures.

Lakmal D. Seneviratne (M'05) received the B.Sc. degree in engineering and the Ph.D. degree in mechanical engineering from King's College London, London, U.K.

He is a Professor of Robotics with Khalifa University, Abu Dhabi, United Arab Emirates, on secondment from King's College London, where he is a Professor of Mechatronics. He has authored more than 250 refereed research papers related to robotics and mechatronics. His current research interests include robotics and autonomous systems.

Dr. Seneviratne is a fellow of the Institution of Engineering and Technology and the Institute of Mechanical Engineers.

Kaspar Althoefer (M'03) received the Dipl.Ing. degree in electronic engineering from the University of Aachen, Aachen, Germany, and the Ph.D. degree in electronic engineering from King's College London, London, U.K.

He is currently the Head with the Centre for Robotics Research, Department of Informatics, King's College London, where he is a Professor of Robotics and Intelligent Systems. He has authored and co-authored more than 200 refereed research papers related to mechatronics, robotics, and intelligent systems.